Pergamon

Geochimica et Cosmochimica Acta, Vol. 59, No. 1, pp. 161–175, 1995

0016-7037/95 $9.50 + .00

0016-7037(94)00231-2

Origin and history of impact-melt rocks of enstatite chondrite parentage

TIMOTHY J. MCCOY,[1] KLAUS KEIL,[1,8] DONALD D. BOGARD,[2] DANIEL H. GARRISON,[3] IGNACIO CASANOVA,[4,7]
MARILYN M. LINDSTROM,[2] ADRIAN J. BREARLEY,[5] KARL KEHM,[6]
ROBERT H. NICHOLS JR.,[6] and CHARLES M. HOHENBERG[6]

[1]Hawaii Institute of Geophysics and Planetology, School of Ocean and Earth Science and Technology, University of Hawaii at Manoa, Honolulu, HI 96822, USA
[2]NASA Johnson Space Center, Code SN-4, Houston, TX 77058, USA
[3]Lockheed-ESC, NASA Johnson Space Center, Code SN-2, Houston, TX 77058, USA
[4]Department of Geology, Field Museum of Natural History, Chicago, IL 60605-2496, USA
[5]Institute of Meteoritics, Department of Earth and Planetary Sciences, University of New Mexico, Albuquerque, NM 87131, USA
[6]McDonnell Center for the Space Sciences, Physics Department, Washington University, St. Louis, MO 63130, USA
[7]Department of the Geophysical Sciences, University of Chicago, Chicago, IL 60605-2496, USA
[8]Hawaii Center for Volcanology, University of Hawaii at Manoa, Honolulu, HI 96822, USA

(*Received December* 28, 1993; *accepted in revised form September* 1, 1994)

Abstract—We have conducted petrologic, chemical, and isotopic studies of two impact-produced rocks of enstatite chondrite parentage. Ilafegh 009 is a total impact-melt rock with no residual lithic clasts. Formation on the EL chondrite parent body is suggested by its mineralogy and mineral compositions. Cooling of the impact melt was rapid at melt temperatures and decreased at subsolidus temperatures. In contrast to previous studies, we show that Happy Canyon is not a new enstatite achondrite but an impact-melt breccia of enstatite chondrite (and not aubrite) parentage. This rock formed by impact melting and incorporation into the melt of clastic material (which resulted in relatively rapid cooling at all temperatures). Mineralogical and bulk compositional data (probably biased by the heterogeneous nature of this rock) do not allow unequivocal determination of its parent body (i.e., EL vs. EH), although some data such as bulk total Fe content seem to favor EL parentage. Both rocks were subjected to post-solidification shock, which was more severe for Ilafegh 009 than for Happy Canyon. It appears that both impact melt rocks could have formed by impact melting ~4.57 Ga ago, as is indicated by the nearly identical I-Xe closure ages of 1.6 and 1.4 Ma before Bjurböle for Ilafegh 009 and Happy Canyon, respectively. An apparently younger ^{39}Ar-^{40}Ar age of 4.53 Ga for Happy Canyon may be due to small biases in the intercalibration of the I-Xe and ^{39}Ar-^{40}Ar chronometers, whereas the much younger 4.34-4.44 Ga age for Ilafegh 009 reflects thermal resetting during shock metamorphism. Shallowater, which was impact-derived from a different enstatite achondrite parent body, has an I-Xe closure age 0.4 Ma younger than that for Ilafegh 009 and an ^{39}Ar-^{40}Ar age of 4.53 Ga. The ancient ages of these three rocks attest to the intense, early bombardment in this region of the solar system.

INTRODUCTION

The enstatite meteorite clan includes diverse, highly reduced chondritic and achondritic rocks. Studies of these meteorites have resulted in the recognition that they are samples from at least four parent bodies (e.g., Keil, 1989, and references therein). Enstatite chondrites are samples from two unmelted parent bodies, the EH and EL bodies. The third, the aubrite parent body, experienced total melting, inefficient metal segregation, crystallization and, possibly, catastrophic fragmentation and gravitational reassembly, resulting in the formation of brecciated rocks composed of mineral and lithic clasts of igneous origin (Okada et al., 1988; Keil, 1989; Casanova et al., 1993a,b). A fourth parent body is represented by the unbrecciated Shallowater enstatite achondrite, which is thought to have formed by impact between a molten and a solid, enstatite meteorite-like planetesimal (Keil et al., 1989).

Here we report the results of petrologic, chemical, and isotopic studies of two additional enstatite meteorites, Ilafegh 009 and Happy Canyon, whose origins have been uncertain and controversial; we also report isotopic results on Shallowater (Kehm et al., 1993). Ilafegh 009 was first interpreted as an L group enstatite chondrite of petrologic type 6 or 7 (EL6; EL7) (Otto, 1992) and later as an impact-melt rock from the EL chondrite parent body (Bischoff et al., 1992; McCoy et al., 1992). Happy Canyon has been interpreted as a new type of enstatite achondrite (Olsen et al., 1977). We elaborate on the impact-melt origin of Ilafegh 009 and show that Happy Canyon is an impact-melt breccia of enstatite chondrite parentage and not a new type of aubrite. However, bulk and mineralogic data do not allow unequivocal assignment of the rock to either the EL or EH parent body, although some data such as bulk total Fe favor EL parentage. We suggest that both formed by impacts early in the history of the solar system. We also show that Shallowater is a very ancient rock, attesting to the intense, early bombardment in the region of the solar system where enstatite-dominated parent bodies formed.

ANALYTICAL TECHNIQUES

Preliminary petrographic examination of Ilafegh 009 was conducted on polished thin section UH 130. This revealed the unusual nature of the meteorite and prompted us to organize a consortium study, for which a large, triangular piece of the meteorite measuring 5.5 × 4.5 cm was obtained. Polished thin section UH 160 was prepared for petrographic studies (note that all polished thin sections used in this study were prepared with alcohol, not water, to avoid loss of water-soluble minerals). A separate section was prepared for

TEM studies. Interior pieces were distributed as follows: 690 mg for I-Xe age dating; 200 mg for oxygen isotopic analysis; 300 mg for Ar-Ar age dating; and 860 mg for bulk analysis by INAA.

We conducted a preliminary study of Happy Canyon using a polished thin section (labelled Wayside 'B') from the collection of the late Glenn I. Huss (this section was also studied by Olsen et al., 1977). We also macroscopically studied a large (15.5 × 7 cm) slab of Happy Canyon from the Huss collection in which we discovered light and dark areas. Polished thin section UH 181 was prepared from the dark material, and UH 182 from the light material. A sample of the dark material (315 mg) was used for Ar-Ar age dating.

Polished thin sections were examined in transmitted and reflected light and photographed using a Nikon photomicroscope. Analyses of individual phases were performed on a Cameca Camebax electron microprobe operated at 15 keV accelerating voltage and an absorbed current of 15 nA (10 nA for plagioclase). A 5 μm beam was used for plagioclase analyses. Natural and synthetic standards of well-known compositions were used and data were corrected using a ZAF program.

Samples of Happy Canyon (59 mg), Ilafegh 009 (98 mg), and Shallowater (107 mg) were irradiated with neutrons in separate packages at the Los Alamos National Laboratory, for the purpose of determining ^{39}Ar-^{40}Ar ages. Also irradiated were samples of terrestrial hornblende NL-25, whose age of 2.65 Ga is believed to be known to better than 1%. Stepwise temperature extractions were made in a high vacuum induction furnace equipped with a thermocouple, and the Ar isotopes released were measured on a mass spectrometer. Corrections were made for extraction blanks, radioactive decay, and reactor-produced interferences. Errors reported for individual ages include uncertainties in these corrections plus analytical uncertainties in measuring the $^{39}Ar/^{40}Ar$ ratios in the samples and the hornblende neutron fluence monitors. Measured irradiation constants, J, determined from multiple hornblende samples are: for the Shallowater irradiation, 520.9 ± 1.0, 519.6 ± 1.5 and 519.2 ± 0.8; for the Ilafegh 009 irradiation, 497.9 ± 0.6, 497.0 ± 1.2 and 495.7 ± 0.5; and for the Happy Canyon irradiation, 334.3 ± 0.6 and 339.4 ± 0.6 (all J values and uncertainties have been multiplied by 10^4). The precision of our determinations of the irradiation constants are much better than 1% for Shallowater and Ilafegh 009, and ~±1% for Happy Canyon. Additional descriptions of reactor corrections applied to the data and of the suitability of the flux monitor used are presented in Bogard et al. (1994).

The I-Xe studies were carried out on a 45.35 mg sample of Ilafegh 009 and a 46.00 mg sample of Shallowater. These samples, together with a whole rock reference sample of the chondrite Bjurböle, were sealed under vacuum in individual quartz vials and neutron irradiated (fluence ≈2 × 10^{19} n/cm^2 at the University of Missouri Research Reactor). After irradiation, each sample was weighed, wrapped in Pt foil, and loaded into the remote arms of a low-blank sample system. The noble gases were extracted from each sample by stepwise heating to progressively higher temperatures in a tungsten coil, with the released gases purified by exposure to SAES St707 getter pellets and freshly deposited Ti films. Xenon was then separated from the other noble gases by selective adsorption onto activated charcoal which was maintained at −70°C, whereas the lighter noble gases were pumped away. The charcoal was then heated, releasing the Xe for analysis. Due to the open coil structure, the indicated temperatures overstate the actual sample temperatures by as much as 200°C. The largest component in both Xe spectra is iodine-derived ^{129}Xe from the decay of extinct ^{129}I, and ^{128}Xe from neutron capture on ^{127}I. Minor amounts of trapped Xe (acquired at formation) are also present, along with smaller contributions from fission and spallation. The high concentrations of radiogenic ^{129}Xe relative to trapped Xe for both Shallowater and Ilafegh 009 present an opportunity to study the I-Xe isotopic structure of these objects with unusually high precision.

Bulk major and trace element compositions of two splits of Ilafegh 009 weighing 71.50 and 63.25 mg, respectively, were determined by INAA using typical procedures currently in use at the NASA Johnson Space Center. The splits were packaged in pure silica tubes and irradiated for 20 hours in a flux of 5.5 × 10^{13} n cm^{-2} s^{-1} at the Research Reactor Facility of the University of Missouri. The samples were counted at about 0.5, 1, 5, and 19 weeks after irradiation in order to obtain data for nuclides with differing half-lives. Details of standards used and data reduction procedures are given by Mittlefehldt and Lindstrom (1991) and Mittlefehldt et al. (1992).

Several grains of enstatite which exhibit optical evidence of a striated microstructure were selected for transmission electron microscope study. Slotted copper grids were glued over the grains of interest, using an acetone insoluble epoxy. After immersion in acetone for 5–8 hours, the samples could be easily removed from their glass mounting slides. These samples were subsequently prepared for transmission electron microscope studies by conventional ion-beam milling techniques, using a Gatan ion beam mill. Transmission electron microscopy was carried out on a JEOL 2000FX analytical transmission electron microscope operated at 200 keV.

PETROLOGY AND GEOCHEMISTRY

Ilafegh 009

Recovery and initial description

A single stone of 421 grams was recovered in October, 1989, in the Algerian Sahara Desert (Otto, 1992). In this initial description, the quasi igneous texture, the presence of nearly cm-sized enstatite crystals, and the lack of chondrules were noted. Mineral compositions suggested a close link to EL chondrites, and the meteorite was classified as an EL chondrite of petrologic type 6 or 7, reflecting what was presumed to be a high degree of metamorphism (Otto, 1992). More detailed investigations showed that Ilafegh 009 is not an ultrametamorphosed chondrite but, rather, an impact-melt rock from the EL chondrite parent body (Bischoff et al., 1992; McCoy et al., 1992).

Texture

In hand-specimen we noticed that Ilafegh 009 is unlike any other enstatite chondrite in that it is light-colored, whereas all enstatite chondrites are dark, presumably because of the smaller average grain sizes of minerals (particularly the opaques). In thin section, no relict chondrules are observed, and the meteorite is dominated by large (up to 0.75 cm in length), interlocking, hypidiomorphic laths of orthoenstatite,

FIG. 1. Photomicrograph of Ilafegh 009, which consists of hypidiomorphic laths of enstatite (e), interstitial opaques (o) (mostly metallic Fe,Ni and troilite, with minor schreibersite, ferroan alabandite and daubréelite), and plagioclase (p). Opaque phases were trapped between the growing enstatite laths, producing a range of unusual shapes. Opaque inclusions in enstatite are also noted. Reflected, plane polarized light. Scale bar = 200 μm.

Table 1. Compositions (in wt.%) of silicate phases in the EL6 impact-melt rock Ilafegh 009 and impact-melt breccia Happy Canyon.

	Ilafegh 009		Happy Canyon							
			Fine-Grained Clasts			Coarse-Grained Melt				Megacryst
Oxide	Enstatite	Plagioclase	Enstatite	Diopside	Plagioclase	Enstatite	Plagioclase	SiO_2	"Granitic"	Enstatite
SiO_2	60.6	64.8	59.7	56.4	62.3	60.4	65.9	97.3	77.1	60.4
	0.38	*1.8*	*0.49*	*0.37*	*1.2*	*0.16*	*0.65*	*0.17*	*0.98*	*0.46*
Al_2O_3	0.24	21.3	0.15	0.71	23.0	0.11	20.9	2.20	12.2	0.18
	0.05	*0.98*	*0.06*	*0.09*	*0.63*	*0.02*	*0.51*	*0.04*	*0.22*	*0.01*
FeO	0.13	0.11	0.37	0.86	1.13	0.29	0.75	0.71	0.37	0.15
	0.08	*0.08*	*0.18*	*0.52*	*0.78*	*0.08*	*0.17*	*0.10*	*0.10*	*0.05*
MgO	37.9	b.d.	39.4	20.2	0.07	39.9	0.04	b.d.	0.48	39.6
	0.37		*0.06*	*0.28*	*0.06*	*0.10*	*0.01*		*0.02*	*0.25*
CaO	0.89	4.27	0.33	23.2	5.44	0.37	3.11	b.d.	0.53	0.93
	0.19	*1.06*	*0.03*	*0.38*	*0.60*	*0.03*	*0.29*		*0.03*	*0.04*
Na_2O	b.d.	9.27	n.a.	n.a.	8.58	n.a.	9.80	1.27	5.64	n.a.
		0.46			*0.47*		*0.14*	*0.26*	*0.19*	
K_2O	n.a.	0.54	n.a.	n.a.	0.40	n.a.	0.64	b.d.	2.77	n.a.
		0.13			*0.06*		*0.05*		*0.08*	
Total	99.76	100.29	99.95	101.37	100.95	101.07	101.14	101.48	99.09	101.26
N	20	9	3	4	10	6	4	3	3	5
		$An_{19.7}Or_{3.0}$			$An_{25.4}Or_{2.2}$		$An_{14.4}Or_{3.5}$			

n.a., Not Analyzed; b.d., Below Detection; N, Number of Analyses
Italicized figures are 1σ of compositional variability.

with interstitial opaque phases (metallic Fe,Ni, schreibersite, troilite, alabandite), and plagioclase (Fig. 1). This intergrowth results in a variety of shapes, including highly irregular outlines where enstatite invades the metal; triangularly-shaped metal trapped between three intersecting enstatite crystals; and laths of metal trapped between two parallel enstatite crystals (Fig. 1). Undulatory extinction and planar fractures are common features of the pyroxene, and some of the large laths have a striated appearance. Individual enstatite crystals also contain abundant inclusions, which are rounded or irregular and range in size from a few to hundreds of μm. Some inclusions consist of plagioclase ± metal ± troilite. A second type of inclusion is K-rich (~7% K_2O) and sometimes contains grains of an SiO_2 phase (Bischoff et al., 1992). Oldhamite was noted by Bischoff et al. (1992), but not observed in our thin sections.

Mineralogy and mineral compositions

Modal analysis of polished thin section UH 160 reveals (in wt%) 52.4 orthoenstatite, 1.9 striated enstatite, 7.1 plagioclase, 27.2 metal + schreibersite, 8.1 titanian troilite + daubreélite, and 0.5 ferroan alabandite. Three grains of osbornite (TiN), about 10–20 μm in size, were identified microscopically. All are enclosed in enstatite and two occur together with plagioclase in melt inclusions. Despite being a find, the metal-sulfides are quite unweathered, presumably because of the meteorite's arid find site. No diopside was observed as either separate grains or as exsolution lamellae in orthoenstatite, and forsterite is absent. Striated enstatite appears to be very heterogeneously distributed, and while it comprises 1.9 wt% of UH 160, we were unable to identify it in polished thin section UH 130. Ilafegh 009 contains much higher abundances of metal and troilite than aubrites (Watters and Prinz, 1979). The abundance of metal is even higher than observed in any EH chondrite and most EL chondrites, with the exception of the EL chondrite Ufana (Keil, 1968). The presence of ferroan alabandite links Ilafegh 009 to the EL chondrites, since this phase is absent from EH chondrites which contain niningerite instead (Keil, 1968).

The compositions of silicate and opaque minerals (Tables 1, 2) are similar to those of EL and different from those of EH chondrites (Keil, 1968). We recognize that comparison of mineral compositions in Ilafegh 009 and EL chondrites may be problematic. Minerals in Ilafegh 009 crystallized from a relatively quickly cooled melt, whereas those from ELs represent solid state equilibration at about 900°C (Keil, 1989). However, in spite of these uncertainties, some of the elemental abundances in minerals for Ilafegh 009 are close to those of ELs, suggesting that the target rock was probably of EL composition and that crystallization of the impact melt took place under O fugacity conditions similar to those prevailing during formation and metamorphism of the EL target rock. For example, average compositions of pyroxene (0.13% FeO, 0.89% CaO), metal (1.0% Si), and plagioclase ($Ab_{77.4}An_{19.7}Or_{2.9}$) are close to those of ELs, although plagioclase is somewhat higher in An and lower in Ab and Or than are average ELs (Keil, 1968). This suggests that vapor fractionation as a result of superheating during impact melting may have depleted the melt in Na and K relative to Ca. No compositional differences are observed between orthoenstatite and striated enstatite, and all metallic Fe,Ni is kamacite. Troilite contains an average of 0.92% Ti, somewhat higher than that of average ELs (~0.6% Keil, 1968). This is possibly due to the fact that in the EL target material, Ti may be present in phases other than troilite (e.g., osbornite). During impact melting and subsequent crystallization, all Ti may be partitioned into troilite, thus slightly increasing its content over that of average ELs. Our analyses of ferroan alabandite differ from those of Bischoff et al. (1992) and have higher Fe (17.3 vs. 14%) and Mg (3.7 vs. 2.3%), but are within the range of analyses of ferroan alabandite from ELs.

Schreibersite is particularly important since it may provide information about the cooling rate of Ilafegh 009 at subsolidus

temperatures. Schreibersite has highly variable Ni contents between grains, with two distinct populations of grains with Ni contents from 6.8–9.4 wt% and 18.7–21.7 wt%. Within individual schreibersite grains of both populations, we observe well-defined gradients in Ni content. In one grain with a diameter of 125 μm, Ni concentrations range from 7.3–9.4 wt%. The presence of well-defined Ni gradients suggests that the formation of schreibersite is controlled by diffusion. Thus, information may be available about the subsolidus cooling history of Ilafegh 009. Schreibersite grains in the size range of 60–250 μm which exhibit Ni gradients from 7–9 wt% suggest cooling rates of about 600°C/1000 yrs (Randich and Goldstein, 1978). However, this cooling rate is affected by considerable uncertainties. This is because it is based on large extrapolations in both Ni content and phosphide size from the model of Randich and Goldstein (1978), and because their model does not consider the effects of minor elements like Si on the cooling rates. Despite these uncertainties, schreibersite compositions suggest relatively rapid cooling at low temperatures.

Bulk composition

We have determined the abundances of nineteen elements in two bulk samples of Ilafegh 009 (Fig. 2, Table 3). We have normalized these data to average EH and EL abundances (Wasson and Kallemeyn, 1988). The composition of Ilafegh 009 is very roughly chondritic, with all elements ranging between 0.3–1.9 times chondritic. This suggests that no extreme igneous fractionation has occurred, consistent with the interpretation that Ilafegh 009 is an impact-melt rock and did not crystallize from an internally-derived, igneous melt. However, there are some notable deviations from chondritic values which may shed light on both the precursor of Ilafegh 009 and the processes operating during the impact.

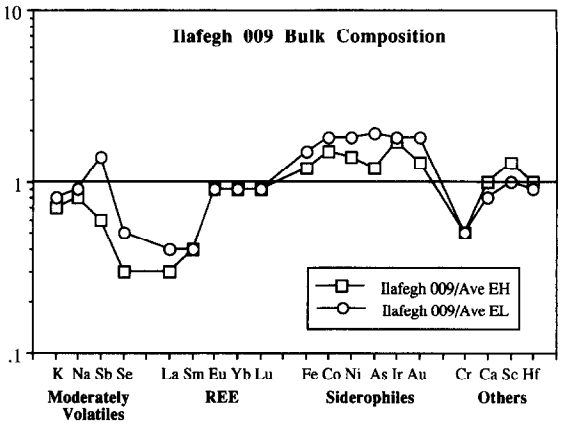

FIG. 2. Bulk composition of Ilafegh 009 relative to average EL and EH chondrites (data from Wasson and Kallemeyn, 1988).

Moderately volatile elements (K, Na, Sb, and Se, in order of increasing volatility) exhibit significant depletions when compared to EH and EL chondrites (Fig. 2, Table 3). These depletions may be due to vapor fractionation as a result of superheating of the impact melt. Element abundances decrease systematically with increasing volatility relative to EH chondrites (K, 0.7; Na, 0.8; Sb, 0.6; Se, 0.3), while they are more variable compared to EL chondrites (K, 0.8; Na, 0.9; Sb, 1.4; Se, 0.5). One possible interpretation of these data is that the precursor of Ilafegh 009 was EH-like, and that the depletions now observed reflect increasing volatility of these elements. However, S is more volatile than these elements and, curiously, is not depleted in Ilafegh 009 (8.1 wt% troilite + daubreelite) relative to either EH (5.8–9.9 wt%; Keil, 1968) or average EL chondrites (5.0–18.3 wt%; Keil, 1968; the meteorite with the extremely high S content may be an

Table 2. Compositions (in wt.%) of opaque minerals in the EL impact-melt rock Ilafegh 009 and the impact-melt breccia Happy Canyon.

	Ilafegh 009					Happy Canyon	
Element	Metal	Schreibersite	Troilite	Daubreelite	Alabandite	Metal	Troilite
Fe	91.8	72.8	60.4	18.1	17.2	91.9	56.8
	0.81	*5.69*	*0.36*	*0.57*	*0.85*	*0.51*	*0.58*
Ni	6.59	12.2	b.d.	b.d.	b.d.	6.25	n.a.
	0.08	*6.2*				*0.10*	
Co	0.30	0.18	n.a.	n.a.	n.a.	0.30	n.a.
	0.03	*0.08*				*0.03*	
Cr	b.d.	b.d.	1.59	34.6	0.22	b.d.	4.15
			0.16	*0.69*	*0.06*		*0.43*
Si	1.02	0.07	n.a.	n.a.	n.a.	0.80	n.a.
	0.01	*0.02*				*0.01*	
P	0.17	14.3	n.a.	n.a.	n.a.	0.47	n.a.
	0.02	*0.16*				*0.02*	
S	n.a.	n.a.	36.6	43.4	37.6	n.a.	37.1
			0.35	*0.21*	*0.13*		*0.84*
Ti	n.a.	n.a.	0.92	0.15	b.d.	n.a.	0.93
			0.02	*0.08*			*0.06*
Mn	n.a.	n.a.	0.10	1.72	41.0	n.a.	n.a.
			0.02	*0.11*	*0.94*		
Ca	n.a.	n.a.	b.d.	b.d.	0.33	n.a.	n.a.
					0.09		
Mg	n.a.	n.a.	b.d.	b.d.	3.68	n.a.	n.a.
					0.20		
Total	99.88	99.55	99.61	97.97	100.03	99.72	98.98
N	10	19	10	10	5	10	5

b.d., below detection; n.a., not analyzed; N, number of analyses
Italicized figures are 1σ of compositional variability.

Table 3. Bulk composition data for two splits of Ilafegh 009 as determined by instrumental neutron activation analysis.

Element	Unit	Split A	Split B	Ave.	Ave./EL[1]	Ave./EH[1]
Na	wt.%	0.484±0.008	0.557±0.009	0.521	0.9	0.8
K	wt.%	0.061±0.014	0.051±0.017	0.056	0.8	0.7
Ca	wt.%	<1.21	0.81±0.21	0.81[2]	0.8	1.0
Sc	ppm	6.95±0.08	7.59±0.08	7.27	1.0	1.3
Cr	ppm	1724±20	1562±18	1643	0.5	0.5
Fe	wt.%	37.2±0.5	30.4±0.4	33.8	1.5	1.2
Co	ppm	1358±15	1097±12	1227	1.8	1.5
Ni	ppm	26300±600	21500±500	23900	1.8	1.4
As	ppm	4.43±0.31	3.93±0.31	4.18	1.9	1.2
Se	ppm	7.4±0.6	6.6±0.6	7.0	0.5	0.3
Sb	ppm	0.139±0.022	0.112±0.022	0.127	1.4	0.6
La	ppm	0.061±0.014	0.084±0.015	0.073	0.4	0.3
Sm	ppm	0.046±0.006	0.068±0.006	0.057	0.4	0.4
Eu	ppm	0.050±0.008	0.050±0.007	0.050	0.9	0.9
Yb	ppm	<0.33	0.15±0.04	0.15[2]	0.9	0.9
Lu	ppm	0.018±0.006	0.023±0.006	0.021	0.9	0.9
Hf	ppm	0.14±0.05	<0.28	0.140[2]	0.9	1.0
Ir	ppb	1040±30	842±78	942	1.8	1.7
Au	ppb	459±8	373±6	416	1.8	1.3

[1] Data for average EL and EH chondrites from WASSON and KALLEMEYN (1988).
[2] Average taken as the only significant analysis.

anomaly). Furthermore, it is interesting to note that chalcophilic elements such as Sb, Se, and Cr are significantly depleted relative to EH and EL chondrites. Thus, one might think that they may have been removed from the impact melt with an immiscible sulfur-rich melt. However, depletion of Sb, Se, and Cr by factors of 2–3 relative to EH or EL target material would require removal of 50–66 wt% of the original sulfur-rich phases. As noted above, this seems unlikely, based on the high abundance of troilite and daubréelite in Ilafegh 009. Thus, the depletion of moderately volatile elements and Cr in Ilafegh 009 remains enigmatic.

Large deviations from chondritic abundances are observed in the siderophile elements (Fig. 2, Table 3). When compared to average EL chondrites, siderophile elements (e.g., Co, Ni, Au, Ir) in Ilafegh 009 are uniformly enriched (1.8 × EL). Siderophile elements are also enriched relative to EH chondrites (1.3–1.7 × EH), although the enrichments are less dramatic and quite variable. These enrichments are consistent with the observation that Ilafegh 009 contains more modal metal and schreibersite (27.2 wt%) than any EH chondrite (18.6–24.1 wt%; Keil, 1968) and most EL chondrites (1.6–28.6 wt%; Keil, 1968). While it is possible that this metal was introduced into the Ilafegh 009 impact melt from the projectile, we consider this unlikely since there is no obvious evidence for mixing of a foreign component. It is possible that Ilafegh 009 inherited its siderophile element enrichment from a metal-rich precursor. This might suggest formation of Ilafegh 009 from EH rather than EL material, based on the overall enrichment of siderophiles in EH relative to EL chondrites. However, we note that the average for EL chondrites (Wasson and Kallemeyn, 1988) does not include data for metal-rich EL chondrites. The EL chondrite Ufana contains more modal metal (28.6 wt%) than any other EL chondrite (Keil, 1968) or Ilafegh 009. Thus, siderophile element abundances do not provide unequivocal information which allows discrimination between an EL or EH chondritic target material, but they are consistent with the proposal that Ilafegh 009 could have formed from the impact melting of a particularly metal-rich EL target material. Perhaps the most likely explanation for the high siderophile contents in Ilafegh 009 is that in the impact melting process, some metal segregated from the target material, and that Ilafegh 009 represents this metal-rich portion. Study of impact melt rocks has shown that such metal segregations are common in impact melts (e.g., Bogard et al., 1995).

The REEs (Fig. 2, Table 3) La and Sm are present at 0.4 × EL, whereas Eu, Yb, and Lu are present at approximately chondritic levels (0.9 × EL). The absence of data on Gd prevents us from distinguishing whether the pattern is gently sloping (Lu/La ~ 2) and has a positive Eu anomaly, or whether there is a depletion in the LREE but not the HREE. The origin of the shape of this REE abundance pattern is uncertain. We do not believe that it was inherited from the precursor target rock, since neither EL nor EH chondrites exhibit such patterns. Fractionation of silicates in the impact melt is possible, but appears unlikely. Pyroxenes are typically LREE-depleted, but absolute REE concentrations in pyroxenes are quite low, requiring an unrealistically large degree of pyroxene fractionation. Fractionation of LREE-enriched plagioclase would almost certainly result in a negative Eu anomaly in the residue (Ilafegh 009), but no evidence for a negative Eu anomaly is noticeable in the REE data. It is possible that oldhamite plays a major role in determining the REE pattern of Ilafegh 009, since it is the major carrier of REEs. We did not observe oldhamite in our samples, perhaps as a result of weathering. We do not, however, believe weathering can explain the REE pattern, since weathering does not change the shape of the REE pattern of oldhamite (Wheelock et al., 1994). It is possible that oldhamite in Ilafegh 009 has a pattern like that in the bulk rock, not unlike weathered oldhamite H-5 studied by Floss et al. (1990), and that it dominates the bulk rock REE pattern.

Oxygen isotopic composition

The oxygen isotopic composition of a whole-rock sample (Ilafegh 009-2d2) is $\delta^{18}O = 5.58$, $\delta^{17}O = 2.86$. Another sample of Ilafegh 009, provided by A. Bischoff, was analyzed and

FIG. 3. Low magnification transmission electron microscope (TEM) image of a region of low-Ca pyroxene which optically exhibits a striated microstructure, showing lamellae parallel to (100), indicative of an intergrowth of two phases. The inset electron diffraction pattern (top right) is consistent with orthoenstatite, but the intensity of alternate diffraction maxima in the pattern are higher, indicating that a phase with a 0.9 nm repeat is present, i.e., clinoenstatite. The holes in the crystal (white) are due to inclusions which have been preferentially lost during ion milling.

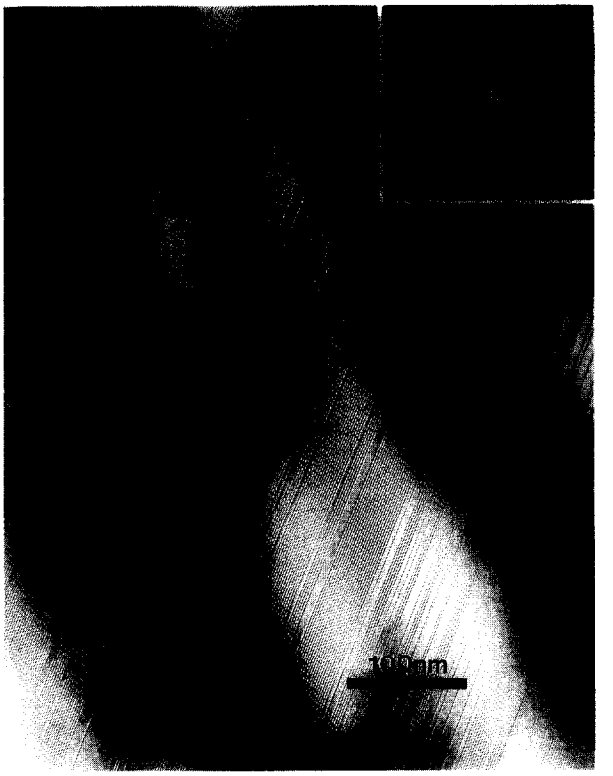

FIG. 4. Higher magnification TEM image of a region of low-Ca pyroxene containing intergrown lamellae of ortho- and clinoenstatite with variable widths. The inset electron diffraction pattern shows evidence of only extremely weak streaking parallel to a^*, showing that the clinoenstatite lamellae are extremely rare and that most lamellae are sufficiently thick to diffract coherently.

yielded $\delta^{18}O = 5.43$, $\delta^{17}O = 2.90$. These two results are well within analytical uncertainty of each other and are similar to mean compositions for EH and EL chondrites and aubrites (Clayton et al., 1984). Thus, they link Ilafegh 009 to the enstatite meteorite clan, but do not allow discrimination between an origin on the EH, EL, or aubrite parent bodies.

Shock effects

Ilafegh 009 has experienced a post-solidification shock event. Enstatite grains exhibit ubiquitous undulatory extinction and planar fractures. Additionally, some enstatite grains are striated parallel to the direction of elongation. We have examined several such striated low-Ca pyroxene crystals by transmission electron microscopy in order to shed light on the formation of this microstructure, i.e., whether it is the result of shock or of rapid cooling. Such data can provide important insights into how the striated microstructure formed. Our studies show that the pyroxene consists of a disordered mixture of both orthorhombic and monoclinic polymorphs. A low magnification image of a region of a pyroxene grain showing its striated microstructure is shown in Fig. 3. The pyroxene is dominantly orthopyroxene, and the occurrence of clinopyroxene is extremely heterogeneous, although locally its abundance may be extremely high. Figure 4 shows a high resolution image of a typical region of pyroxene which consists of lamellae of orthopyroxene and clinopyroxene, but is dominated by orthopyroxene. The lamellae of both phases have variable widths (Fig. 5), but in most cases are relatively thick (20–40 nm). Very thin lamellae are present, but their abun-

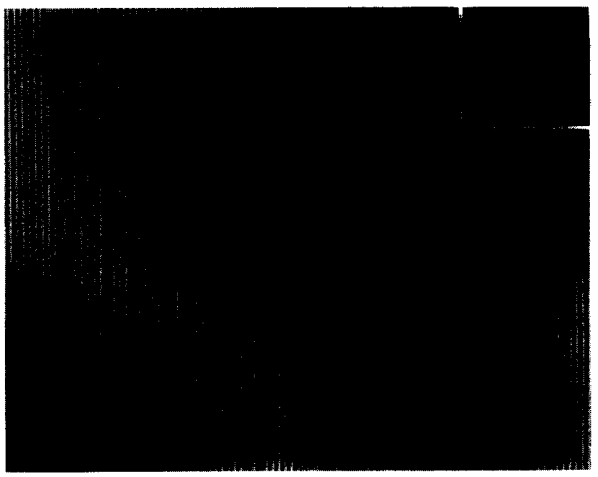

FIG. 5. High resolution (TEM) image of the low-Ca pyroxene showing thick intergrown lamellae of both ortho- and clinoenstatite. A few thin lamellae of clinoenstatite, typically two unit cells in thickness, are indicated by arrows.

dance is relatively low, as indicated by the lack of streaking in electron diffraction patterns (insert in Fig. 5). We have measured the thicknesses of the clinopyroxene lamellae from several regions of these intergrowths directly from high resolution transmission electron micrographs. A histogram of the lamellae width (in unit cells parallel to the a axis) vs. frequency is shown in Fig. 6. The most important observation from these data is that the lamellae widths are all even multiples of the 0.9 nm (100) repeat of the pyroxene. This puts important constraints on the origin of the intergrowths.

Disordered low-Ca pyroxenes can form by a number of different mechanisms, depending on their thermal histories. Three possible mechanisms have been discussed in the literature (Buseck et al., 1982). These are first, inversion from protoenstatite during cooling from high temperature; second, inversion due to shear, either homogeneous or inhomogeneous (shock); and third, inversion from orthoenstatite as a result of annealing within the clinoenstatite stability field. A fourth mechanism, annealing of clinoenstatite within the orthoenstatite stability field, is also a possibility. The microstructural data discussed above can be used to distinguish between these mechanisms. The possibility that the clinoenstatite formed by inversion from protoenstatite during cooling from high temperature (mechanism 1) can be ruled out unequivocally. As pointed out by Buseck and Iijima (1975), disordered intergrowths formed by this process can have clinoenstatite lamellae thicknesses which are both odd and even multiples of the 0.9 nm clinoenstatite *a*-repeat. The Ilafegh 009 striated enstatite has lamellae widths which are only even multiples (Fig. 6). In addition, the microstructures of pyroxenes produced by cooling of protoenstatite from high temperatures through the orthoenstatite inversion temperature are entirely different from those observed in Ilafegh 009 (Jones and Brearley, 1992; Brearley and Jones, 1993). Enstatite produced by slow cooling, consisting dominantly of orthoenstatite, exhibits an evenly distributed disorder in the product phase, not a heterogeneous distribution such as that observed in Ilafegh 009. In addition, the maximum lamellae width of clinopyroxene in this material is 10 unit cells, not up to 100 unit cells such as in Ilafegh 009.

The fourth mechanism, annealing of clinoenstatite within the orthoenstatite stability field, can be ruled out because it can also result in a disordered intergrowth which contains clinoenstatite lamellae with widths that are both odd and even multiples of the 0.9 nm *a*-repeat, contrary to what is observed in Ilafegh 009.

The second and third mechanisms, inversion due to shock or as a result of annealing of orthoenstatite in the clinoenstatite stability field, cannot be distinguished by the lamellae widths alone, because both result in clinoenstatite lamellae which are only even multiples of the clino *a*-repeat. However, other arguments can be presented against inversion by annealing of orthopyroxene and indicate that shock is the most likely mechanism of formation of the striated enstatite in Ilafegh 009. The idea that clinoenstatite could form from inversion of orthoenstatite comes largely from experimental data (Grover, 1972). These observations indicate that there may be a low temperature stability field (<556°C) for clinoenstatite at 1 atm. However, there is considerable discussion as to whether such a stability field does, in fact, exist and most

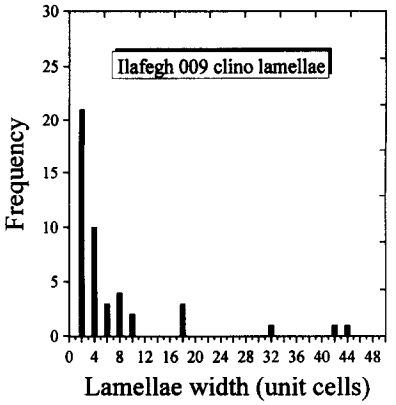

FIG. 6. Diagram showing the frequency distribution of different clinoenstatite lamellae widths in striated enstatite from Ilafegh 009. In all cases, the lamellae widths are even multiples of the 0.9 nm (100) (*a*) repeat of clinoenstatite.

authors regard clinoenstatite as being metastable at low temperatures. In addition, there is essentially no geological evidence which would indicate that this reaction occurs in terrestrial rocks, even those which have experienced extended thermal histories and often in the presence of water, which would catalyze phase transformation. This suggests that the reaction is extremely sluggish on geological timescales. These data argue strongly against the third mechanism for the development of the disordered intergrowths in Ilafegh 009. We conclude that the intergrowth of orthoenstatite and clinoenstatite in Ilafegh 009 formed by shock. This conclusion is consistent with several petrographic features of this meteorite, including the presence of undulatory extinction and planar fracture. In addition, the heterogeneous development of clinoenstatite in orthopyroxene and the fact that some grains which are highly striated often show evidence of kinking can only be reasonably reconciled with a shock origin.

Origin of Ilafegh 009

Although unequivocal identification of the target rock that was melted by impact to form Ilafegh 009 is difficult, we suggest that, considering all data obtained in this study, it appears that it may have been EL material. Ilafegh 009 crystallized from a total impact melt and, thus, no relict clasts exist whose study would allow identification of the target material. However, the oxygen isotopic composition and highly reduced mineralogy of the rock indicate that its parent material belongs to the enstatite chondrite/aubrite clan, and the presence of abundant metal eliminates aubrites as source and, rather, suggests a chondritic target rock of the EH or EL type (an origin on the Shallowater parent body is not likely because the mineral inclusions in enstatite of Ilafegh 009 are different from those in Shallowater). Bulk composition provides only ambiguous clues as to whether the target was of the EH or EL type. The high siderophile element contents are consistent with either EH or EL classification, and neither the volatile element nor the REE contents allow distinction between an EH or EL target. However, compositions of some minerals (e.g., presence of niningerite; CaO and FeO of pyroxene; Si of metallic Fe,Ni) are consistent with the sugges-

tion that the target rock was either a metal-rich EL chondrite not unlike the chondrite Ufana (Keil, 1968), or that in the impact melting process of EL material, some local metal segregation took place, and Ilafegh 009 is a sample of such a portion of the impact melt. Thus, we classify Ilafegh 009 as an impact melt from the EL parent body.

Happy Canyon

Previous work

An extensive study of this meteorite has previously been conducted by Olsen et al. (1977), who concluded that the rock was a new type of enstatite achondrite. However, our study of their thin section and of additional sections and a large hand-specimen yields very different results and conclusions. The previous work (Olsen et al., 1977) correctly points to close affinities of the meteorite to EL chondrites, based on mineral and bulk compositions, although the lack of Si in the metallic Fe,Ni claimed by Olsen et al. (1977) suggested to them that the rock formed under higher O fugacity then EL chondrites. However, we find typical amounts of Si in the metallic Fe,Ni (Table 2), and the link of Happy Canyon to EL chondrites is, therefore, not in doubt. The affinity of the rock to enstatite meteorites has also been confirmed by oxygen isotopic analyses (Mayeda and Clayton, 1980). Based on the uniform distribution and size of enstatite crystals, Olsen et al. (1977) correctly note that Happy Canyon is an igneous rock that crystallized from a melt, but the lack of partially resorbed olivine suggested to them that it crystallized under high pressure, possibly in the core volume of an asteroid. However, they failed to recognize the significance of the various lithologies described below (which do occur in their thin section as well as ours), which provide convincing evidence that the rock is an impact-melt breccia that cooled rapidly from high temperature, thus eliminating any concern for the presence of unresorbed olivine and the need for crystallization under high pressure deep within an asteroid. We, therefore, conclude that Happy Canyon is not a new type of enstatite achondrite but, rather, an impact-melt breccia from the EL chondrite parent body. It should be noted that Rubin (1985) previously suggested that the meteorite is an impact melt rock.

Hand-sample description

Macroscopic examination and study with a low-power stereomicroscope of a slab of 15.5 × 7 cm in size reveals a subtle light-dark structure, with light and dark, swirly portions intermingling, not unlike what is seen in chondritic impact-melt breccias (Rubin, 1985; Bogard et al., 1995). Furthermore, despite extensive terrestrial alteration of metallic Fe,Ni and FeS (Happy Canyon is a weathered find), these phases are clearly recognizable in hand-specimen and preferentially occur at its edge, closest to the fusion crust. It appears that these phases must have been mobile and were concentrated near what are now the edges of the slab. This segregation of metal and troilite on a cm scale is also typical for chondritic impact-melt breccias (e.g., Bogard et al., 1995).

Petrography, mineralogy, and mineral composition

Our microscopic study of thin sections (including the one studied by Olsen et al., 1977) shows the occurrence of three lithologies. The most abundant (~70 vol%) is a *coarse-grained,* equigranular lithology dominated by enstatite, whereas a *fine-grained* lithology comprises approximately 30 vol% of the rock (Fig. 7a). Large enstatite *megacrysts,* which enclose other phases, are a third lithology and make up less than 1 vol% of the meteorite (Fig. 7b).

The *coarse-grained* lithology is dominated by enstatite, which occurs as subhedral grains of relatively uniform size (~100–300 μm) and distribution (Fig. 7a). Minor phases (<5 vol% each) include distinct, subhedral grains of plagioclase and SiO_2, as well as metallic Fe,Ni and sulfides; one grain of osbornite, 15 × 30 μm in size, was found and is partially rimmed by troilite. In one of three thin sections examined in the electron microprobe, a material of granitic composition occurs as an interstitial phase. The texture of this lithology indicates that it formed by crystallization from a

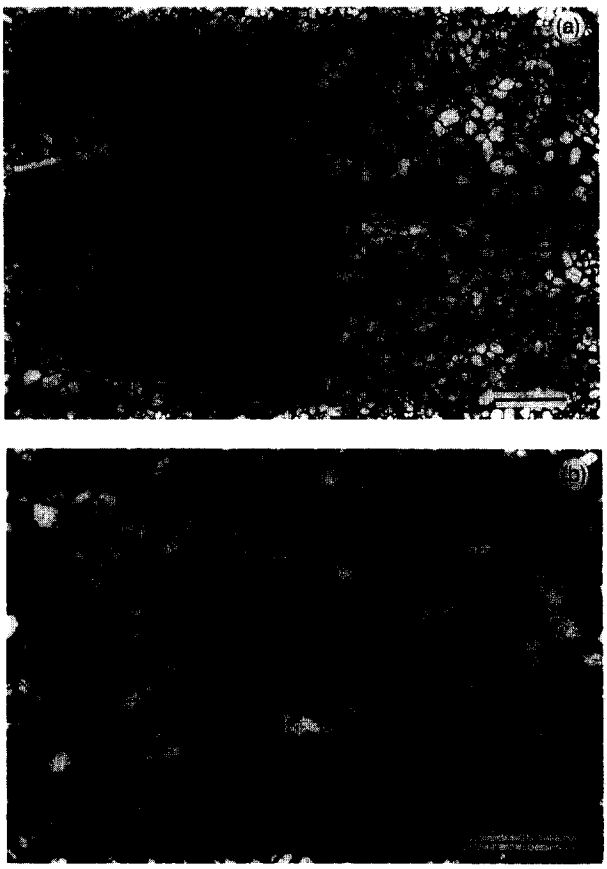

FIG. 7. Transmitted, plane polarized light photomicrographs of Happy Canyon. (a) The coarse-grained lithology (right) is dominated by equant enstatite crystals of uniform size and distribution and comprises ~70 vol% of the rock. We interpret this lithology as the product of crystallization from an impact melt. The fine-grained lithology (center left) always occurs surrounded by the coarse-grained lithology and represents relict material of the parent target rock. Scale bar = 1 mm. (b) One of the large megacrysts that comprise ~1% of the rock, which always occur either within the coarse-grained lithology (as in this Fig.), or on the boundaries of coarse- and fine-grained lithologies. Scale bar = 1 mm.

melt. Compositions of minerals in this lithology (Table 1) are similar to those in EL6s (in parentheses, data from Keil, 1968, for EL6s): enstatite has 0.29% FeO (0.18%); plagioclase is $An_{14.4}$ ($An_{15.0}$); metallic Fe,Ni has 0.80% Si (1.3%); and troilite has 0.93% Ti (0.65%). SiO_2 occurs in the highly recrystallized EL6s, but granitic material has not been reported. However, in contrast to EL6s, metallic Fe,Ni has 0.47% P and lacks exsolved schreibersite, and troilite has 4.15% Cr and no daubréelite exsolution lamellae. We conclude that the Happy Canyon impact-melt breccia cooled relatively fast, even at low temperatures, so that P and Cr remained in solution in their host minerals and did not exsolve as schreibersite and daubréelite, respectively.

The *fine-grained* lithology occurs as distinct patches up to 5 mm in diameter and is enclosed within the coarse-grained lithology. Its texture can best be described as that of a metamorphosed rock, with distinct subhedral grains of enstatite and diopside and interstitial grains of plagioclase (due to terrestrial weathering, this is not readily visible in transmitted light in Fig. 7a, but is clearly discernable in reflected light in the microscope). The average grain size of this lithology is 68 μm (σ = 38, N = 20), which is slightly finer-grained than that of the EL6 chondrite Hvittis (110 μm, σ = 76, N = 19). This might indicate that the target rock for Happy Canyon had not been metamorphosed to petrologic type 6. Enstatite is by far the dominant phase (90 vol%), and its composition is similar to that of EL6s. Plagioclase is significantly more anorthitic ($An_{25.4}$) than that of any of the EL6s studied by Keil (1968) (up to $An_{16.6}$), and diopside occurs in this lithology, but is unknown from EL6s; one grain of osbornite, 12 μm in size, was found enclosed in enstatite. We interpret this lithology to represent metamorphosed, clastic target material that was engulfed in the impact melt (the coarse-grained lithology) during impact melting. This is indicated by similarities in average grain sizes and textures (notably the presence of discrete grains of enstatite with interstitial plagioclase) between this lithology and EL6 chondrites. We recognize that diopside, which is present in this lithology, is unknown from EL chondrites and that the plagioclase composition differs significantly from those of EL6s. Perhaps this is because EL6 chondrites in the world's collections do not represent the entire spectrum of material present on the EL parent body, or because this material was compositionally altered during the impact event.

Megacrysts of enstatite (not mentioned by Olsen et al., 1977) are up to 5 mm in length and somewhat skeletal in appearance (Fig. 7b) and, although heavily fractured, appear to originally have been single crystals. They are present in all thin sections studied, and they occur either included within the coarse-grained lithology (as in Fig. 7b) or at the boundary between coarse- and fine-grained lithologies, but never within the fine-grained lithology. Small (10–40 μm) inclusions of metallic Fe,Ni, plagioclase, and diopside are observed within the megacrysts, although these are too weathered for reliable microprobe analysis. The megacrysts have CaO contents (0.93%) higher than that of enstatite in the coarse-grained (0.37%) and fine-grained (0.33%) lithologies, but similar to that of EL6s (0.74%; Keil, 1968). We suggest that these megacrysts formed early by spontaneous crystallization from the supercooled impact melt which then continued to crystallize the coarse-grained lithology.

Shock effects

Enstatite in all three lithologies exhibits undulatory extinction. There is no evidence for higher degrees of shock in any one lithology when compared to the other two. Thus, the entire meteorite was subjected to a shock event after solidification which affected all three lithologies to the same degree, but Happy Canyon is clearly less shocked than Ilafegh 009.

Origin of Happy Canyon

Our studies suggest that Happy Canyon is not a new type of enstatite achondrite (Olsen et al., 1977), but an impact melt-breccia of enstatite meteorite parentage, in agreement with the earlier suggestion of Rubin (1985). The occurrence of clastic material (the fine-grained lithology) within the melt portion (the coarse-grained lithology) is strong evidence that the rock formed by impact melting and engulfment of unmelted target rock. Cooling of the impact-melt breccia appears to have been rapid, probably as the result of incorporation of cold, clastic target material (the fine-grained lithology) into the impact melt. That cooling was rapid is evidenced by the limited segregation of metallic Fe,Ni-sulfides in the melt portion (movement over less than a few cm), and the lack of schreibersite exsolution from metal and daubréelite exsolution from troilite. After solidification, the entire rock was shocked by yet another impact event, as is indicated by the undulatory extinction of the enstatite.

However, the question on which parent body this rock formed by impact melting is much more difficult to answer. The high contents of metallic Fe,Ni and bulk Fe appear to eliminate the aubrite parent body as a source for Happy Canyon. Furthermore, the texture and the lack of the typical Shallowater xenolith assemblage within enstatite (Keil et al., 1989) of Happy Canyon suggests that it is not related to Shallowater. Olsen et al. (1977) concluded that Happy Canyon is closely related to EL chondrites, based on the bulk Fe content. Mineral compositions in the three Happy Canyon lithologies are not unequivocal indicators of either EL or EH parentage, although the Si content of metallic Fe,Ni is within the range of that of EL chondrites. Thus, we conclude that Happy Canyon is clearly of enstatite chondrite parentage and, possibly, formed on the EL body, but origin from an EH source cannot be ruled out with confidence.

ISOTYPE CHRONOLOGY

In this section we present the K-Ar and I-Xe chronology of Ilafegh 009, Happy Canyon, and Shallowater. Previous I-Xe studies suggest that Shallowater is also an ancient rock (Hohenberg, 1967), and petrologic studies suggest that it too formed by impact-related processes. While Ilafegh 009 and Happy Canyon formed by impact into a solid target(s), Shallowater formed when two enstatite planetesimals, one molten and the other solid, collided and mixed (Keil et al., 1989). Thus, Shallowater formed on a different parent body and under different circumstances than Ilafegh 009 and Happy Canyon. Nevertheless, Shallowater can provide important in-

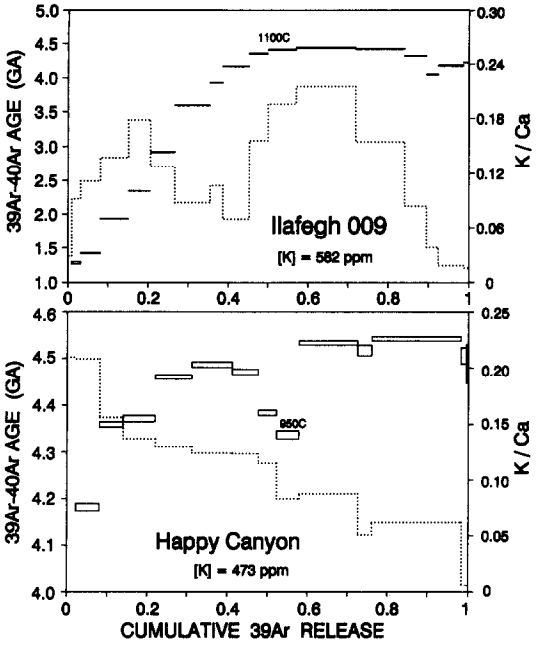

FIG. 8. ^{39}Ar-^{40}Ar ages (rectangles and solid lines) and K/Ca ratios (dotted lines) as a function of cumulative release of ^{39}Ar for stepwise temperature extractions of Ilafegh 009 and Happy Canyon. Individual age uncertainties are indicated by the width of the rectangle. Potassium concentrations and the temperature releasing 50% of the total ^{39}Ar are also indicated for each meteorite.

sights into the early chronology of enstatite-dominated parent bodies and, thus, we include Shallowater in this discussion.

^{39}Ar-^{40}Ar Ages

Calculated ^{39}Ar-^{40}Ar ages and K/Ca ratios for each temperature extraction of Ilafegh 009 and Happy Canyon are shown as a function of cumulative ^{39}Ar release in Fig. 8. An analogous plot for Shallowater is shown in Fig. 9. Interpretation of these age spectra requires consideration of the evidence that different K-bearing mineral phases degas Ar as a function of stepwise extraction temperature. All three meteorites release ^{39}Ar and ^{40}Ar in two broad peaks at temperatures of ~800 and ~1200-1300°C. This is illustrated for Ilafegh 009 and Shallowater in Fig. 10; Happy Canyon shows a very similar release profile. Ilafegh 009 and Shallowater also show two distinct peaks in K/Ca ratios, which approximately correspond to the two ^{39}Ar release peaks. Although stepwise temperature extractions of meteorites commonly show phases with distinct K/Ca ratios, it is unusual for these distinct phases to have similar K/Ca. Happy Canyon shows the more typical (although modest) decrease in K/Ca with increasing temperature. The high-temperature peak in the K/Ca release for Ilafegh 009 is probably caused by microscopic inclusions of plagioclase and K-feldspar contained within enstatite grains, as described earlier and reported by Bischoff et al. (1992). The K/Ca ratios for Ilafegh 009 (Fig. 8) are similar to those for plagioclase in this meteorite (Table 1). The K/Ca ratios shown during temperature release of Shallowater (Fig. 9), however, fall between ratios measured for oligoclase (0.146) and anorthoclase (31.2), as reported by Keil et al.

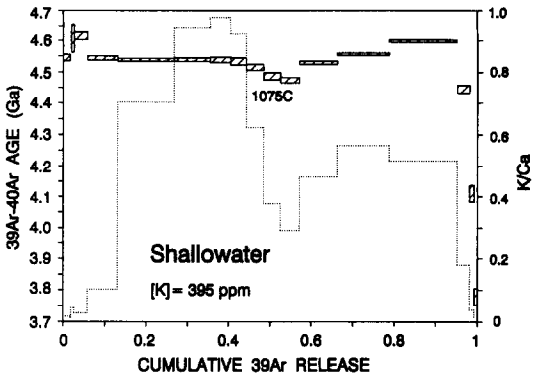

FIG. 9. ^{39}Ar-^{40}Ar ages (rectangles) and K/Ca ratios (dotted lines) as a function of cumulative release of ^{39}Ar for stepwise temperature extractions of Shallowater. Individual age uncertainties are indicated by the width of the rectangle. The potassium concentration and the temperature releasing 50% of the total ^{39}Ar are also indicated.

(1989). Shallowater also has inclusions of various phases, including feldspars, contained within the enstatite crystals (Keil et al., 1989).

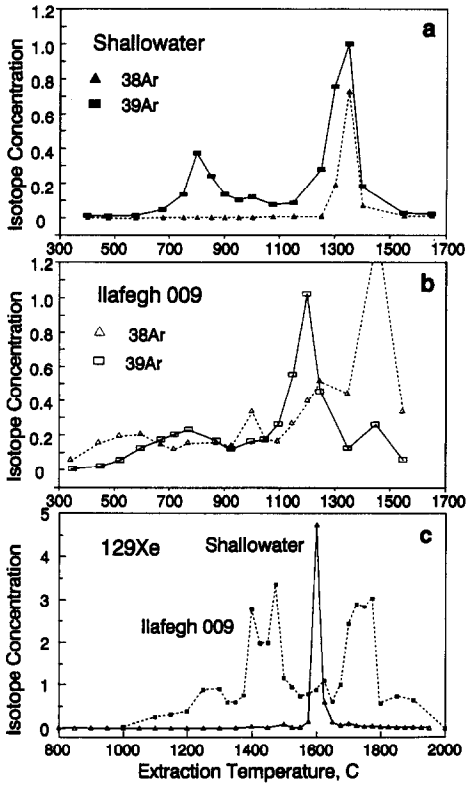

FIG. 10. Stepwise temperature release of ^{38}Ar (units of 10^{-6} cm^{3}STP/g) and ^{39}Ar (units of 10^{-7} cm^{3}STP/g) from Shallowater (a) and Ilafegh 009 (b) and of ^{129}Xe (c) from Shallowater (units of 10^{-10} cm^{3}STP/g) and Ilafegh 009 (units of 10^{-11} cm^{3}STP/g). Release of ^{128}Xe is essentially identical to that of ^{129}Xe. Isotopes ^{39}Ar, ^{38}Ar, and ^{129,128}Xe monitor lattice sites for K, Cl, and I, respectively. All Ar concentrations have been normalized to 100°C temperature intervals. The apparent extraction temperatures for the Xe from Shallowater and Ilafegh 009 correspond to the coil temperature and probably overstate the actual sample temperatures by as much as 200–300°C.

Although most of the K in Ilafegh 009 probably resides in feldspar, the ^{39}Ar and ^{40}Ar released from the inclusions is forced to diffuse through large enstatite grains. Because studies of chondrites commonly show that Ar releases more readily from the high K/Ca phase (probably feldspar) than from the low K/Ca phase (mafic minerals), the ^{39}Ar-^{40}Ar ages of these inclusions are likely to be more difficult to reset by heating. The entire low-temperature phase of Ilafegh 009 shows lowered ages that are consistent with recent diffusive loss of radiogenic ^{40}Ar. (Both Ilafegh 009 and Happy Canyon are weathered finds). The high-temperature phase, however, appears to have retained its Ar and gives an average age of 4.34 Ga (for eight extractions with cumulative $^{39}Ar > 45\%$). The oldest ages shown by this phase are 4.42–4.44 Ga (two extractions releasing 27% of the ^{39}Ar). We conclude that the time of major Ar degassing of Ilafegh 009 is somewhat uncertain and probably lies between 4.34–4.44 Ga.

Compared to Ilafegh 009, Happy Canyon shows much less ^{40}Ar loss at low extraction temperatures and older ^{39}Ar-^{40}Ar ages at high temperatures. This age profile is qualitatively similar to data of lesser resolution reported by Kennedy (1981). The total age of Happy Canyon is 4.43 Ga and would be a lower limit to the time of major Ar degassing. The high-temperature phase (as defined by the ^{39}Ar release profile) suggests an approximate plateau age of 4.53 ± 0.02 Ga for five extractions releasing ~40% of the ^{39}Ar. (Where the age is weighed by the amount of ^{39}Ar released, but the quoted uncertainty is the standard deviation of the simple mean.) The slight decrease in ^{39}Ar-^{40}Ar age at the highest extraction temperatures is associated with a phase with low K/Ca ratio of ~0.02; these ages may have been altered by neutron-induced recoil of ^{39}Ar from feldspar into this high-temperature phase. Our data suggest loss of small amounts of ^{40}Ar from low-retention sites in both the low-temperature and the high-temperature phase (e.g., the 950°C data). Weathering of grain surfaces of different K-bearing phases may explain this effect. In spite of evidence for modest ^{40}Ar diffusive loss, we interpret the high-temperature age plateau of 4.53 ± 0.02 Ga to represent the last major Ar degassing event of Happy Canyon, presumably the impact melting event.

Shallowater shows no evidence for recent loss of ^{40}Ar. Its total ^{39}Ar-^{40}Ar age is 4.53 ± 0.05 Ga (where the uncertainty is the standard deviation of the mean of all extractions, except the two highest extractions). The average age of the low-temperature phase is 4.54 Ga and is essentially identical to the average age of 4.53 Ga for the high-temperature phase. An isochron plot (not shown here) of $^{40}Ar/^{36}Ar$ vs. $^{39}Ar/^{36}Ar$ is highly linear ($\chi^2 = 0.967$), passes through the origin (indicating the absence of ^{40}Ar not associated with K), and gives an age of 4.55 ± 0.05 Ga. The five extractions releasing 6–45% of the ^{39}Ar define a constant or plateau age of 4.539 ± 0.003 Ga. However, several individual ^{39}Ar-^{40}Ar ages, all associated with low K/Ca ratios, show variations outside of these analytical uncertainties. The decrease in age for the three highest temperature extractions is probably an effect due to ^{39}Ar recoil; the age decrease at 50–55% ^{39}Ar release possibly has the same cause as the similar decrease in Happy Canyon. No evidence exists in the Ar isotopic data that the slightly higher ages at 2–6% ^{39}Ar release are due to adsorbed atmospheric ^{40}Ar; they may be due to preferential leaching of K from grain surfaces. We infer that the closure time for the K-Ar system in Shallowater occurred 4.53 ± 0.03 Ga ago.

The inferred ^{39}Ar-^{40}Ar ages for Happy Canyon and Shallowater, 4.53 ± 0.02 and 4.53 ± 0.03 Ga, respectively, are the same. The ^{39}Ar-^{40}Ar degassing age for Ilafegh 009 appears to be distinctly younger than that of Happy Canyon, and is similar to the ^{39}Ar-^{40}Ar age determined for the St. Marks EH5 enstatite chondrite (Bogard and Garrison, 1991). The ^{39}Ar-^{40}Ar ages for Happy Canyon and Shallowater rank among the oldest precise K-Ar ages for meteorites. We recently reported a ^{39}Ar-^{40}Ar age of 4.52 ± 0.01 Ga for the acapulcoite Monument Draw, which is believed to have reached metamorphic temperatures near melting on its parent body (Bogard et al., 1993). Unshocked ordinary chondrites typically show ^{39}Ar-^{40}Ar ages of 4.42–4.52 (Turner et al., 1978), the younger ages probably being due to Ar diffusive loss during parent body metamorphism. Essentially all eucrites show ^{39}Ar-^{40}Ar ages of ~3.4–4.2 Ga, and these are interpreted to represent resetting by large impacts on the HED parent body (Bogard and Garrison, 1992). However, even the old ^{39}Ar-^{40}Ar ages of Happy Canyon and Shallowater appear younger than some meteorite formation times of 4.55–4.56 Ga determined by other chronometers (e.g., Prinzhofer et al., 1992).

I-Xe Chronology

In I-Xe dating the association of ^{128}Xe, from n-capture on ^{127}I in the reactor, with radiogenic ^{129}Xe, from the decay of now extinct ^{129}I, is used to establish the initial iodine isotopic ratio at the time of Xe closure $(^{129}I/^{127}I)_0$. Since the half-life of ^{129}I is relatively short (17 Ma) with respect to solar system timescales, this initial ratio changes rapidly in the early solar system, making it a sensitive chronometer for dating Xe closure in the iodine host phase. The intimate association of these iodine-derived isotopes required for I-Xe dating is best displayed as a three-isotope correlation diagram (Fig. 11) in which $^{128}Xe/^{132}Xe$ is plotted against $^{129}Xe/^{132}Xe$ for the Xe released in stepwise heating. The linear relationships (isochrons) demonstrate that only two Xe components are present, a trapped component at the bottom left and a single I-derived component at the upper right, implying a fixed ratio of ^{129}Xe to I-derived ^{128}Xe. This ratio, given by the isochron slope, is proportional to a unique value of $(^{129}I/^{127}I)_0$ and, thus, provides the Xe closure time for the sample. While the value of $(^{129}I/^{127}I)_0$ can, in principle, be directly calculated from the isochron using an accurate knowledge of the neutron irradiation parameter (e.g., Hohenberg and Kennedy, 1981), it is more convenient (and probably more precise), to include a standard reference sample, typically the L4 chondrite Bjurböle, in each irradiation. The relative I-Xe ages between closure in the I-bearing host phases in the samples studied and in the reference sample are then given simply by differences in their isochron slopes. Apparent I-Xe age variations due to small gradients in the neutron fluence (<5%) are small (<80,000 years) compared to the precision of the isochrons.

The radiogenic ^{129}Xe release patterns for Shallowater and Ilafegh 009 are plotted vs. extraction temperature in Fig. 10 (note that these patterns are essentially identical for those for radiogenic ^{128}Xe, which are, therefore, not plotted). The extraction temperatures cited here are the temperatures of the

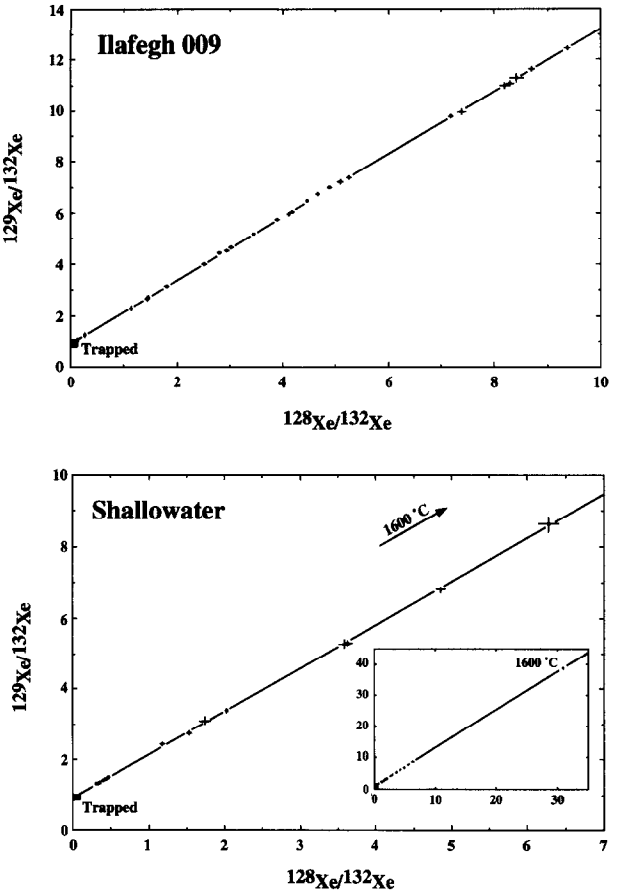

FIG. 11. $^{129}Xe/^{132}Xe$ vs. $^{128}Xe/^{132}Xe$ for the high-temperature extractions for Ilafegh 009 and Shallowater. The isochron for Ilafegh 009 is defined by twenty seven data points (1σ error bars are plotted), which corresponds to ~98% of the radiogenic ^{129}Xe in the sample. The Shallowater isochron is defined by seventeen successive data points, corresponding to ~96% of its radiogenic ^{129}Xe. The isochron lines are least squares free-fits to the data and pass through a typical trapped component (e.g., AVVC, Average Value Carbonaceous Chondrite; Eugster et al., 1967).

tungsten heating coil which probably overstate the actual sample temperatures by as much as 200–300°C. Shallowater displays a prominent release peak at an apparent temperature of ~1600°C which accounts for more than 90% of the radiogenic ^{129}Xe in the meteorite. This peak likely corresponds to the melting of the major mineral, enstatite, indicating that I is probably sited either in the enstatite lattice itself or in inclusions within enstatite. This result is consistent with previous studies which have identified enstatite as the probable carrier of radiogenic ^{129}Xe in enstatite-type meteorites (Crabb and Anders, 1982). In contrast to Shallowater, there are two broad release peaks for Ilafegh 009 at apparent temperatures of ~1450°C and ~1750°C, with each accounting for about 30% of the radiogenic ^{129}Xe. This indicates the presence of at least two major I carriers, which closed to Xe diffusion at the same time. Although the identities of these carriers cannot conclusively be determined from these data, it may be that these correspond to the melting of two different phases associated with enstatite (see below).

The isochrons for Ilafegh 009 and Shallowater are shown in Fig. 11. The quality of these isochrons is among the best observed in I-Xe dating (e.g., Swindle and Podosek, 1988; Swindle et al., 1988), with twenty-seven consecutive temperature fractions defining the isochron for Ilafegh 009 and seventeen fractions defining the isochron for Shallowater, yielding a precision in closure times of approximately ±80,000 years for both meteorites. The differences in the slopes of these two isochrons indicate that Xe closure in Ilafegh 009 occurred about 400,000 years before similar closure in Shallowater. Referencing to the Bjurböle internal irradiation standard shows that Xe closure in Ilafegh 009 occurred 1.6 ± 1.2 Ma before closure in Bjurböle. Kennedy (1981) measured a nearly identical I-Xe age for Happy Canyon (~1.4 Ma before Bjurböle).

Although the I-Xe chronometer has generally been regarded as a relative chronometer, recent inter-calibration with precision Pb-Pb techniques have provided absolute I-Xe ages. Cl-apatites from the Acapulco meteorite have been studied with both Pb-Pb (Göpel et al., 1992) and I-Xe (Nichols et al., 1992), which provide calibration for the phosphates in Acapulco and, by means of the relative I-Xe age, a calibration for Bjurböle. Xenon closure in the major Bjurböle I-host phases occurred at 4.565 ± 0.003 Ga (Nichols et al., 1994). Xenon closure in Ilafegh 009, Happy Canyon, and Shallowater all occurred at very nearly this same time, with relative closure times ~1.5 Ma before Bjurböle. This suite of dates implies that the events that set the I-Xe clock in these meteorites occurred at about the same time, early in the history of their respective parent bodies.

Implications of Chronology

The I-Xe formation intervals for Ilafegh 009, Happy Canyon, and Shallowater are all the same within <1 Ma and, furthermore, are within a few Ma of the formation intervals for a variety of other meteorites (e.g., Swindle and Podosek, 1988). As discussed above, the I-Xe ages measure a time period very early in the history of these enstatite parent bodies, that is ~4.565 Ga ago. For reasons not completely understood, I-Xe formation ages of many meteorites usually do not correlate with absolute ages obtained by various other radiometric methods. In many meteorites, it appears that iodine is incorporated into minor mineral phases formed during secondary processes. Thus, I-Xe dates secondary alteration whereas other chronometers data primary events, explaining the discrepancy between I-Xe and other chronometers (Nichols et al., 1993). This does not, however, appear to be the case for the three meteorites studied here which formed from largely or completely molten systems, with no petrologic evidence for secondary alteration. These melts were produced by impacts for Ilafegh 009 and Happy Canyon and at least partly by endogenic sources for Shallowater (Keil et al., 1989). The evidence (presented below) that the phase being dated by I-Xe for Shallowater is present as inclusions within the enstatite suggests that the system has been protected from chemical alteration. In fact, enstatite meteorites, with their large enstatite crystals, represent one of the few meteorite chemical groups for which the I-Xe chronometer is consistent with chronology inferred from petrological considerations (Kennedy, 1981; Swindle and Podosek, 1988).

The ^{39}Ar-^{40}Ar ages for Happy Canyon and Shallowater, 4.53 ± 0.02 Ga and 4.53 ± 0.03 Ga, respectively, rank among

the oldest ^{39}Ar-^{40}Ar ages for meteorites. Because the K-Ar chronometer is relatively easy to reset, these ages require that impact metamorphism associated with formation of these meteorites occurred very early. Although these ^{39}Ar-^{40}Ar ages appear younger than the I-Xe ages of ~4.566 Ga, this difference is at the assigned $1-2\ \sigma$ level. Furthermore, there exists an additional <1% uncertainty in calibration of the ^{39}Ar-^{40}Ar chronometer due to uncertainties in the absolute age of the NL-25 hornblende monitor. These factors suggest that the differences between the I-Xe and K-Ar ages for Shallowater and Happy Canyon may not be real. The ^{39}Ar-^{40}Ar age for Ilafegh 009, however, appears to be distinctly younger than either the I-Xe or K-Ar ages for the other two meteorites. In this section, we examine some of the possible events in the history of the enstatite parent bodies that determined both the I-Xe and K-Ar ages.

It is important to establish whether the I-Xe and K-Ar chronometers are dating similar phases and, thus, can be directly compared, and whether these phases are primary, i.e., formed directly by crystallization. In the case of Shallowater, Fig. 10 suggests that a common phase was dated. Although ^{39}Ar released from Shallowater occurs in two peaks and ^{129}Xe in only one, the higher temperature peak in the ^{39}Ar release coincides with the peak release of ^{38}Ar, most of which was made in the irradiation by neutron capture on ^{37}Cl. Considering the greater uncertainty in measuring absolute temperatures for Xe extraction, the difference in temperatures of maximum release of $^{38,39}Ar$ and ^{129}Xe are probably not significant. The similarities in release profiles suggest a similar loss mechanism for Ar and Xe from this phase. Because we expect Cl and I to occur together, we conclude that the high-temperature phase in Shallowater represents degassing from K- and I-containing inclusions within enstatite, where diffusion loss of Ar and Xe is controlled by the enstatite. Since the high temperature release peaks for Xe and Ar are so sharp, the release of Ar and Xe is probably not governed by diffusion but by partial melting of the enstatite itself. Although the Ar release temperature of ~1400°C is well below the melting point of pure enstatite (1580°C), melting of plagioclase and enstatite would certainly occur at a lower temperature. This observation is consistent with the observed tracking of I-Xe chronometry of enstatite meteorites with meteorite petrographic classification, as mentioned above. The low-temperature phase of Shallowater that contains K but no halogens is probably feldspar which is located between, not within, large enstatite grains.

It is not as clear whether these two chronometers are dating the same phases in Ilafegh 009 and Happy Canyon. (The I-Xe chronology for the latter was studied by Kennedy, 1981). For Ilafegh 009, the ^{39}Ar, ^{38}Ar, and ^{129}Xe releases are more complex (Fig. 10). Most of the ^{38}Ar and a small amount of ^{39}Ar are released in the 1450°C extraction, which may correspond to the broad release for ^{129}Xe around 1700°C (Fig. 10). Much of the ^{39}Ar and a small amount of ^{38}Ar are released at ~1200°C, which may correspond to the broad ^{129}Xe release peak at 1400–1500°C. (A likely reason for the apparent difference in Ar and Xe degassing temperatures is given in the section on Analytical Techniques). A broad ^{39}Ar peak at 700–800°C and a broad ^{38}Ar peak (terrestrial weathering contamination?) at 500–600°C show no counterpart in ^{129}Xe. Thus, we conclude that part, but not all of the I (represented by ^{129}Xe) and Cl (represented by ^{38}Ar) in Ilafegh 009 are contained within enstatite inclusions which release at high temperatures (~1450°C). Only a modest fraction of the K is associated with this phase, however. Much of the K (^{39}Ar) and a substantial part of the I (^{129}Xe) in Ilafegh 009 are apparently in associated phases releasing at ~1200°C. It is unclear which phases identified petrographically correspond to these two release temperatures. It is possible that much of the I and Cl are in inclusions within the enstatite, whereas much of the K and additional I are in the feldspar. Although the two major Xe release peaks for Ilafegh 009 are separated by about 350°C, they lie on the same I-Xe isochron, suggesting rapid cooling for this temperature range, with a lower limit for the cooling rate of ~5000°C/Ma. For Happy Canyon, almost all of the Cl and I (Kennedy, 1981) and much of the K show release in a broad, possibly double peak at 1000–1400°C. Overall, Fig. 10 suggests that most of the Ar and part of the Xe would be more readily lost from Ilafegh 009 and Happy Canyon compared to Shallowater.

The next step in interpreting the chronologic information is determining exactly what events are being dated. Since Shallowater seems to show the best correlation between release patterns for I-Xe and K-Ar, we will consider it first. It seems likely that formation of these enstatite meteorites from a melt would completely reset the I-Xe systematics at that time, arguing that the melting events must have occurred very early in the history of the solar system (i.e., ~4.566 Ga ago). However, Keil et al. (1989) conclude that the inclusions (including plagioclase) contained within enstatite grains of Shallowater were incorporated as solid xenoliths. Thus, the inclusions may have been closed to I-Xe prior to their incorporation into the enstatite melt and remained closed during this mixing and subsequent cooling history. Thus, the actual time of formation of Shallowater by planetesimal collision might be better represented by the K-Ar age of ~4.53 Ga. This explanation would require that Shallowater cooled sufficiently fast to prevent resetting of the I-Xe system, a possibility we now consider.

Keil et al. (1989) argued that Shallowater experienced a complex cooling history as a consequence of collisional break-up and mixing of material from a solid and molten planetesimal, followed by reassembly of the Shallowater parent body, and later collisional excavation. From considerations of mineral stability and micro-textures, they suggested that Shallowater cooled at a rate exceeding 100°C/hr down to a temperature near 712°C, then annealed down to a temperature of 680°C at a cooling rate no greater than 7.5°C/Ma, followed by fast cooling of >0.4°C/day at temperatures below 680°C. By this model it would have required a time period of ~5 Ma to cool through the ~32°C temperature interval of the second cooling stage. This time interval is too short to be resolved in the ^{39}Ar-^{40}Ar age of Shallowater, but it could be seen in the I-Xe formation interval if Xe diffusion loss still occurred at ~700°C. The fact that the I-Xe formation age for Shallowater is similar to those for Ilafegh 009 and Happy Canyon, but 1.6 Ma older than the determined interval for Bjurböle, suggests that the I-Xe system closed to diffusion prior to this interval of slow cooling.

To evaluate Ar diffusion in Shallowater, we used the stepwise release data of ^{39}Ar to calculate the Ar diffusion param-

eter, D/a^2, as a function of extraction temperature (Fechtig and Kalbitzer, 1966). From these diffusion data for the high-temperature phase, we calculated the closure temperature for Ar diffusion (Dodson, 1973), assuming a cooling rate of 7°C/Ma. The Ar closure temperature obtained, ~665°C, is slightly below the suggested annealing interval and suggests that the K-Ar chronometer would have remained an open-system during the period of slow cooling. (Cooling rates slower than 7°C/Ma would give even lower closure temperatures). If the rate of slow cooling for Shallowater were actually substantially slower than the upper limit of 7°C/Ma, or if the temperature interval for slow cooling were actually greater than the 32°C/Ma estimated by Keil et al. (1989), then this ~5 Ma time interval could become considerably longer. Thus, differences in closure temperatures might explain most or all of the apparent ~35 Ma difference in I-Xe and K-Ar ages.

We cannot make the same comparison for Ilafegh 009 and Happy Canyon, which experienced a different history from Shallowater. Their Xe release curves (Fig. 10) demonstrate that part of the I is contained in two separate phases that lose Xe at appreciably lower and higher temperatures compared with Shallowater. Yet, the I-Xe formation intervals for these three meteorites are nearly identical. These observations strongly suggest that Xe was not lost by slow diffusion, but that the I-Xe formation intervals in all three meteorites were, in fact, established during crystallization of the molten portions of the meteorites. Even though the parent bodies for Ilafegh 009 and Happy Canyon (possibly the EL body) and Shallowater parent bodies are apparently different (Keil et al., 1989; Keil, 1989), these melting events occurred within ~0.5 Ma of one another.

The apparently younger K-Ar ages for Ilafegh 009 and Happy Canyon might be explained by later shock events or through long, post-solidification cooling times. It is clear from our petrologic studies that both meteorites experienced post-solidification shock, and that this shock was more severe in Ilafegh 009. (No post-solidification shock effects are observed in Shallowater; Keil et al., 1989). The fact that Ilafegh 009 is more heavily shocked and shows a significantly lowered age suggests that its younger ^{39}Ar-^{40}Ar age represents thermal resetting about 4.4 Ga ago. Post-solidification shock events were also proposed by Minster et al. (1979) to explain Rb-Sr isochron ages of 4.335 ± 0.050 Ga for the St. Marks and 4.393 ± 0.043 Ga for the Indarch EH enstatite chondrites. The cooling history of Happy Canyon is considerably less certain, but the lack of metal/troilite segregation and lack of schreibersite and daubréelite and the presence of unmelted clasts suggests relatively rapid cooling during its entire thermal history.

In summary, the existence in these meteorites of significant amounts of ^{129}Xe from decay of extinct ^{129}I, and determined I-Xe formation intervals that are very similar to those previously determined for the Bjurböle and Acapulco meteorites imply that the melting events that formed Ilafegh 009, Happy Canyon, and Shallowater occurred shortly after formation of their respective parent bodies. (In the case of Shallowater, which is thought to have formed by collision of a molten and a solid asteroid and subsequent gravitational reaccretion of the debris, melting was concurrent with parent body formation; Keil et al., 1989). The ^{39}Ar-^{40}Ar ages for Happy Canyon and Shallowater at 4.53 Ga appear to be slightly younger than the I-Xe ages. The younger K-Ar ages may not be real but, rather, may reflect small biases in the neutron irradiation monitor or in the ^{39}Ar-^{40}Ar technique compared to other chronometers. On the other hand, if the K-Ar ages are actually younger, they may represent a period of slow cooling for Shallowater and thermal resetting by impact in the case of Ilafegh 009 and possibly Happy Canyon. In any case, the ^{39}Ar-^{40}Ar ages for Shallowater and Happy Canyon rank among the oldest determined and demonstrate that these meteorites experienced no significant thermal events after ~4.53 Ga ago. The significantly younger ^{39}Ar-^{40}Ar age for Ilafegh 009, however, may represent resetting by a later shock event that did not affect the I-Xe. The similarities of I-Xe ages for all three meteorites suggests that this region of the solar system experienced an intense bombardment very early in its history.

CONCLUSIONS

Our studies indicate that Ilafegh 009 is a total impact-melt rock and Happy Canyon is an impact-melt breccia, both of enstatite chondrite parentage. Bulk and mineral compositional data do not allow us to determine with certainty the specific enstatite chondrite parent body on which these rocks formed, although some data suggest it may have been the EL parent body. Their ancient ages attest to the fact that their parent body(ies) was heavily impact-altered early in the history of the Solar System. I-Xe closure ages are essentially the same at 1.6 and 1.4 Ma before Bjurböle for Ilafegh 009 and Happy Canyon, respectively. These ages appear to have been established during impact-melting ~4.566 Ga ago. Ages by ^{39}Ar-^{40}Ar for Happy Canyon appear to be younger at 4.53 Ga ago and are much younger for Ilafegh 009 at 4.34–4.44 Ga ago. The differences between the I-Xe and ^{39}Ar-^{40}Ar chronometers for Happy Canyon and Shallowater may not be real but, rather, may result from slight errors in the intercalibration of the two chronometers. Alternatively, younger K-Ar ages may result from shock resetting and slow cooling, respectively. The much younger ^{39}Ar-^{40}Ar age for Ilafegh 009 seems to result from thermal resetting during a post-solidification shock event. Younger K-Ar ages are consistent with the presence of shock features in both Happy Canyon and Ilafegh 009, with the latter being more severely shocked.

Acknowledgments—We thank G. Huss for the loan of samples and thin sections of Happy Canyon, R. N. Clayton for unpublished oxygen isotopic data for Ilafegh 009, D. Mittlefehldt and R. Martínez for assistance in acquisition of trace element data, and M. Weisberg, T. Swindle, and J. Jones for constructive reviews. This work was supported in part by NASA grants NAG 9-30 and NAGW-3281 (K. Keil), NAG 9-7 (C. Hohenberg), 152-14-40-20 (D. Bogard), and 152-13-40-21 (M. Lindstrom). This is Hawai'i Institute of Geophysics and Planetology Publication No. 786 and School of Ocean and Earth Science and Technology Publication No. 3669.

Editorial handling: C. Koeberl

REFERENCES

Bischoff A., Palme H., Geiger T., and Spettel B. (1992) Mineralogy and chemistry of the EL-chondritic melt rock Ilafegh 009. *Lunar Planet. Sci.* **XXIII**, 105–106. (abstr.)

Bogard D. D. and Garrison D. H. (1991) ^{39}Ar-^{40}Ar dating of three enstatite chondrites and the Shallowater aubrite. *Lunar Planet. Sci.* **XXII,** 115–116. (abstr.)

Bogard D. D. and Garrison D. H. (1992) ^{39}Ar-^{40}Ar ages of howardite clasts: Additional evidence for early HED parent body bombardment. *Lunar Planet. Sci.* **XXIII,** 131–132. (abstr.)

Bogard D. D., Garrison D. H., McCoy T. J., and Keil K. (1993) ^{39}Ar-^{40}Ar ages of acapulcoites and lodranites: Evidence for early parent body heating. *Lunar Planet. Sci.* **XXIV,** 141–142. (abstr.)

Bogard D. D., Garrison D. H., Norman M. D., Scott E. R. D., and Keil K. (1995) ^{39}Ar-^{40}Ar age and petrology of Chico: Large-scale impact melting on the L chondrite parent body. *Geochim. Cosmochim. Acta* (in press).

Brearley A. J. and Jones R. H. (1993) Chondrite thermal histories from low-Ca pyroxene microstructures: Autometamorphism vs. prograde metamorphism revisited. *Lunar Planet. Sci.* **XXIV,** 185–186. (abstr.)

Buseck P. R. and Iijima S. (1975) High resolution electron microscopy of enstatite II: Geological applications. *Amer. Mineral.* **60,** 771–784.

Buseck P. R., Nord G. L., and Veblen D. R. (1982) Subsolidus phenomena in pyroxenes. *Rev. Mineral.* **7,** 117–211.

Casanova I., Keil K., and Newsom H. E. (1993a) Composition of metal in aubrites: Constraints on core formation. *Geochim. Cosmochim. Acta* **57,** 675–682.

Casanova I., McCoy T. J., and Keil K. (1993b) Metal-rich meteorites from the aubrite parent body. *Lunar Planet. Sci.* **XXIV,** 259–260. (abstr.)

Clayton R. N., Mayeda T. K., and Rubin A. E. (1984) Oxygen isotopic compositions of enstatite chondrites and aubrites. *Proc. Lunar Planet. Sci. Conf.* **15th,** *J. Geophys. Res.* **89,** C245–C249.

Crabb J. and Anders E. (1982) On the siting of noble gases in E-chondrites. *Geochim. Cosmochim. Acta* **46,** 2351–2361.

Dodson M. H. (1973) Closure temperature in cooling geochronological and petrological systems. *Contr. Mineral. Petrol.* **40,** 259–274.

Eugster O., Eberhardt P., and Geiss J. (1967) Krypton and xenon isotopic composition in three carbonaceous chondrites. *Earth Planet. Sci. Lett.* **3,** 249–257.

Fechtig H. and Kalbitzer S. (1966) The diffusion of argon in potassium-bearing solids. In *Potassium-Argon Dating* (ed. O. Schaeffer and J. Vahringer), pp. 68–107. Springer Verlag.

Floss C., Strait M. M., and Crozaz G. (1990) Rare earth elements and the petrogenesis of aubrites. *Geochim. Cosmochim. Acta* **54,** 3553–3558.

Göpel C., Manhes G., and Allegre C. J. (1992) U-Pb study of the Acapulco meteorite. *Meteoritics* **27,** 226 (abstr.)

Grover J. E. (1972) The stability of low-clinoenstatite in the system $Mg_2Si_2O_6$-$CaMgSi_2O_6$. *EOS-Trans. Amer. Geophys. Union* **53,** 539. (abstr.)

Hohenberg C. M. (1967) I-Xe dating of the Shallowater achondrite. *Earth Planet. Sci. Lett.* **3,** 357–362.

Hohenberg C. M. and Kennedy B. M. (1981) I-Xe dating: Intercomparisons of neutron irradiations and reproducibility of the Bjurböle standard. *Geochim. Cosmochim. Acta* **45,** 1909–1915.

Jones R. H. and Brearley A. J. (1992) An experimental and TEM investigation of the effect of cooling rate on the proto-to-ortho transition in enstatite. *EOS-Trans. Amer. Geophys. Union.* **73,** 619. (abstr.)

Kehm K., Nichols R. H., Jr., Hohenberg C. M., McCoy T. J., and Keil K. (1993) I-Xe structure of Ilafegh 009 and Shallowater: Evidence for early formation and rapid cooling of impact-derived enstatite meteorites. *Lunar Planet. Sci.* **XXIV,** 777–778. (abstr.)

Keil K. (1968) Mineralogical and chemical relationships among enstatite chondrites. *J. Geophys. Res.* **73,** 6945–6976.

Keil K. (1989) Enstatite meteorites and their parent bodies. *Meteoritics* **24,** 195–208.

Keil K., Ntaflos Th., Taylor G. J., Brearley A. J., Newsom H. E., and Romig A. D., Jr. (1989) The Shallowater aubrite: Evidence for origin by planetesimal impacts. *Geochim. Cosmochim. Acta* **53,** 3291–3307.

Kennedy B. M. (1981) Potassium-argon and iodine-xenon gas retention ages of enstatite chondrite meteorites. Ph.D. dissertation. Washington Univ.

Mayeda T. K. and Clayton R. N. (1980) Oxygen isotopic compositions of aubrites and some unique meteorites. *Proc. Lunar Planet. Sci. Conf.* **11th,** 1145–1151.

McCoy T. J., Keil K., Bogard D., Casanova I., and Lindstrom M. M. (1992) Ilafegh 009: A new sample of the diverse suite of enstatite impact melt rocks. *Lunar Planet. Sci.* **XXIII,** 869–870. (abstr.)

Minster J. F., Ricard L. P., and Allegre C. J. (1979) ^{87}Rb-^{87}Sr chronology of enstatite meteorites. *Earth Planet. Sci. Lett.* **44,** 420–440.

Mittlefehldt D. W. and Lindstrom M. M. (1991) Generation of abnormal trace element abundances in Antarctic eucrites by weathering processes. *Geochim. Cosmochim. Acta* **55,** 77–87.

Mittlefehldt D. W., See T. H., and Hörz F. (1992) Dissemination and fractionation of projectile materials in the impact melts from Wabar Crater, Saudi Arabia. *Meteoritics* **27,** 361–370.

Nichols R. H., Hohenberg, C. M., and Marti K. (1992) ^{129}I-derived and ^{244}Pu-fission Xe in individual neutron-irradiated phosphate crystals from the Acapulco meteorite. *Meteoritics* **27,** 268. (abstr.)

Nichols R. H., Hohenberg C. M., Kim Y., and Marti K. (1994) I-Xe studies of the Acapulco meteorite: absolute I-Xe ages of individual phosphate crystals and of the Bjurböle standard. *Geochim. Cosmochim. Acta* **58,** 2553–2561.

Okada A., Keil K., Taylor G. J., and Newsom H. (1988) Igneous history of the aubrite parent asteroid: Evidence from the Norton County enstatite achondrite. *Meteoritics* **23,** 59–74.

Olsen E. J., Bunch T. E., Jarosewich E., Noonan A. F., and Huss G. I. (1977) Happy Canyon: A new type of enstatite achondrite. *Meteoritics* **12,** 109–123.

Otto J. (1992) New meteorite finds from the Algerian Sahara Desert. *Chem. Erde* **52,** 33–40.

Prinzhoffer A., Papanastassiou D. A., and Wasserburg G. J. (1992) Samarium-neodymium evolution of meteorites. *Geochim. Cosmochim. Acta* **56,** 797–815.

Randich E. and Goldstein J. I. (1978) Cooling rates of seven hexahedrites. *Geochim. Cosmochim. Acta* **42,** 221–233.

Rubin A. E. (1985) Impact melt rocks of chondritic material. *Rev. Geophys.* **23,** 277–300.

Swindle T. M. and Podosek F. A. (1988) Iodine Xenon dating. In *Meteorites and the Early Solar System* (ed. J. F. Kerridge and M. S. Matthews), pp. 1127–1146. Univ. Arizona Press.

Swindle T. D., Caffee M. W., and Hohenberg C. M. (1988) Iodine-xenon studies of Allende inclusions: Eggs and the Pink Angel. *Geochim. Cosmochim. Acta* **52,** 2215–2227.

Turner G., Enright M. C., and Cadogan P. H. (1978) The early history of chondrite parent bodies inferred from ^{40}Ar-^{39}Ar ages. *Proc. Lunar Planet. Sci. Conf.* **9th,** 989–1025.

Wasson J. T. and Kallemeyn G. W. (1988) Compositions of chondrites. *Phil. Trans. Roy. Soc. London* **A325,** 535–544.

Watters T. R. and Prinz M. (1979) Aubrites: Their origin and relationship to chondrites. *Proc. Lunar Planet. Sci. Conf.* **10th,** 1073–1093.

Watters T. R. and Prinz M. (1980) Mt. Egerton and the aubrite parent body. *Lunar Planet. Sci.* **XI,** 1225–1227. (abstr.)

Wheelock M. M., Keil K., Floss C., Taylor G. J., and Crozaz G. (1994) REE geochemistry of oldhamite-dominated clasts from the Norton County aubrite: Igneous origin of oldhamite. *Geochim. Cosmochim. Acta* **58,** 449–458.